# Unravelling the lipocalin 2 interaction with aptamers: may rolling circle amplification improve their functional affinity?

*Ramón Lorenzo-Gómez, Noelia Fernández-Alonso, Rebeca Miranda-Castro, Noemí de-los-Santos-Álvarez, María Jesús Lobo-Castañón**

Dpto. Química Física y Analítica, Universidad de Oviedo, Julián Clavería 8, 33006 Oviedo, Spain.

Instituto de Investigación Sanitaria del Principado de Asturias, Avenida de Roma, 33011 Oviedo, Spain

**Declaration of interests**: none

* Corresponding Author. Email address: mjlc@uniovi.es

**Published:** Talanta 2019, 197, 406-412 (DOI: 10.1016/j.talanta.2019.01.057)

## Novelty statement

A truncated aptamer recognizing the cancer biomarker Lipocalin-2 or NGAL is described. Aptamer binding affinity must be characterized under the conditions of the assay. The immobilization of the target can lead to an increase in its local concentration, which improves the functional affinity of the aptamer. A further improvement of this parameter is achieved by coupling a rolling circle amplification reaction for elongating the aptamer after the affinity interaction.

## Highlights

- Anti-cancer biomarker aptamers are not always well characterized leading to unreliable performance in analytical assays
- Fast isothermal rolling circle amplification (15 min) leads to a $10^3$-fold increase in the functional affinity of the aptamer
- Most favorable interaction on the solid-surface due to increase in the local protein concentration
- Different stability of aptamer-free protein and aptamer-bound protein complexes compromise the efficiency of competitive assays

# *Graphical Abstract (for review)

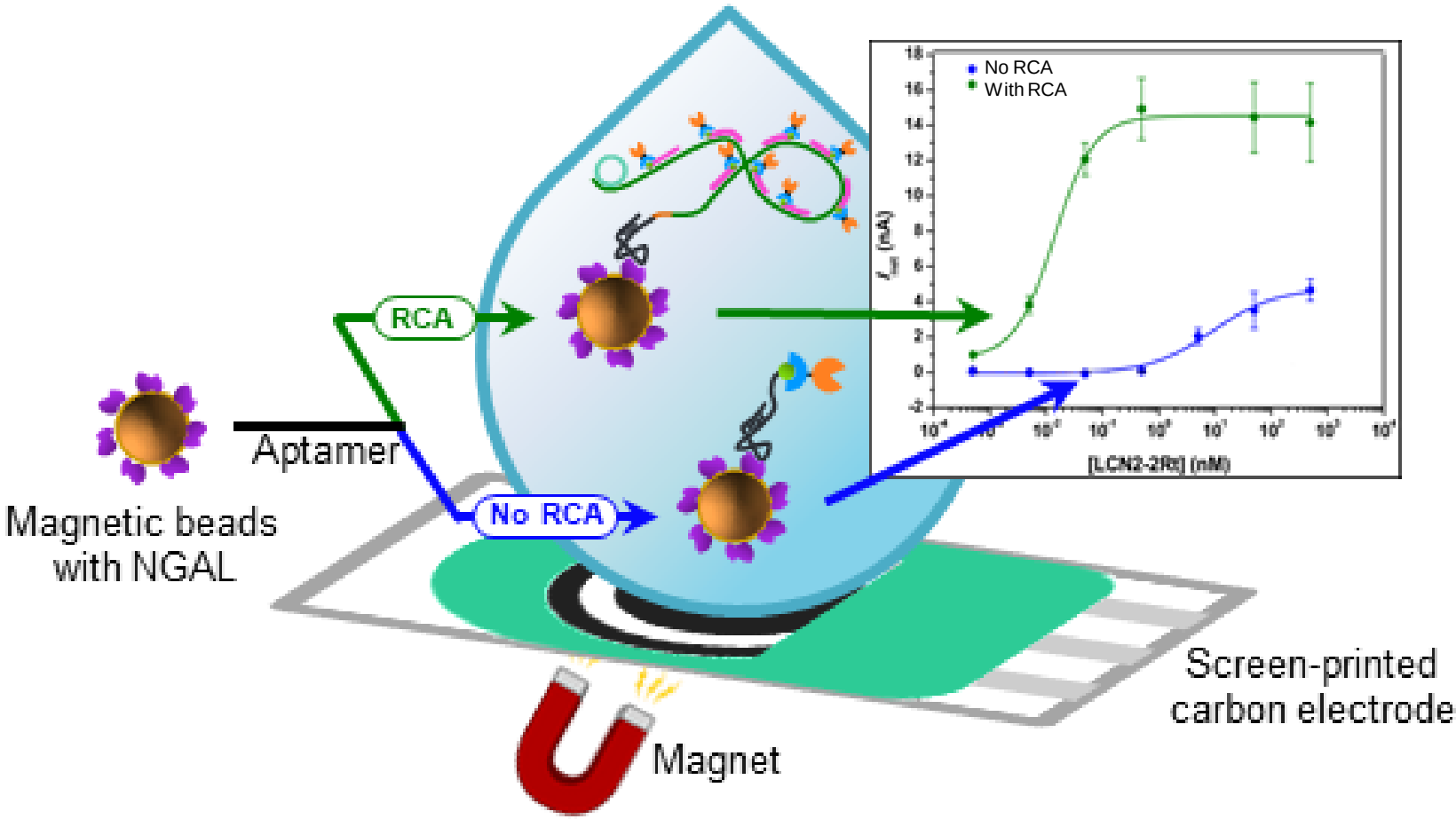

**Abstract**

Cancer diagnosis based on serum biomarkers requires receptors of extreme sensitivity and selectivity. Tunability of aptamer selection makes them ideal for that challenge. However, aptamer characterization is a time-consuming task, not always thoroughly addressed, leading to suboptimal aptamer performance. In this work, we report on the affinity characterization and potential usage of two aptamers against a candidate cancer biomarker, the neutrophil gelatinase–associated lipocalin (NGAL). Electrochemical sandwich assays on Au electrodes and SPR experiments showed a restricted capture ability of one of the aptamers (LCN2-4) and a small detectability of the other (LCN2-2). Interestingly, a truncated version of the signaling aptamer LCN2-2 selectively binds to NGAL covalently linked to magnetic beads due to high local protein concentration. The functional affinity of this aptamer is enhanced by three-orders of magnitude using rolling circle amplification (RCA), completed in only 15 min, followed by hybridization with short complementary fluorescein-tag probes, enzyme labeling and chronoamperometric measurement. Microscale thermophoresis experiments show a poor affinity for the protein in solution, which urges the importance of a full and in-depth characterization of aptamers to be used as diagnostic reagents.

**Keywords**: aptamer characterization, NGAL, electrochemical detection, microscale thermophoresis, rolling circle amplification

## Introduction

Detection of cancer biomarkers in circulation provides an opportunity to achieve an early diagnostic of tumors, increasing the survival rate. Recent studies demonstrate that detection of somatic mutations (liquid biopsies) combined with protein biomarkers increases the sensitivity of current blood tests focused on a single biomarker [1, 2].

Biomarker discovery and clinical validation relies on the availability of highly selective, ideally specific, and sensitive receptors for the recognition of low-abundant biomolecules in biological fluids. Until now, antibodies are the gold standard biomolecules for rapid and sensitive recognition of that exclusive set of cancer-related biomarkers, commonly (glyco)proteins, which have reached the approval status for clinical usage. At present only one of them is valuable for risk assessment (alpha-fetoprotein, AFP-L3%) that is for early diagnostic, while nuclear matrix protein 22 (NMP-22) and certain forms of prostatic specific antigen (PSA) become diagnostic markers. The rest remains after diagnosis markers (prognostic, predictive and pharmacodynamics)[3, 4]. In the search of new and more sensitive and specific biomarkers, detection of a variety of post-translational modifications in proteins exclusive of malignant conditions are gaining importance. The great heterogeneity of those cancer-related changes enforces the receptor molecule to an even superior challenge. As an example, antibodies that recognize glycan moieties are much less abundant than peptide-recognizing counterparts because of the markedly higher immunogenicity of the latter [5].

In such a scenario, the number of aptamers raised against potential cancer biomarkers is increasing not only because their therapeutic applications but also for diagnostic purposes [6, 7]. To the latter aim, aptamers present appealing advantages over antibodies. They can be selected against non-immunogenic or toxic compounds

and interestingly, they are eligible to molecular amplification or recycling schemes forbidden to antibodies to develop ultrasensitive methods of biomarker detection.

Rolling circle amplification (RCA) is an isothermal DNA amplification strategy performed under mild conditions that provides an elongated sequence of tandem repeats of a template that can be exploited for signal amplification. Aptamer tagging with a particular sequence acting as a primer for the circularizable RCA template (also known as padlock) is straightforward at a modest cost, and thus RCA can be used for signal generation in aptamer-based assays, thereby dramatically improving their sensitivity [8, 9]. However, the limit of detection attainable by this approach may depend on the specific affinity of the aptamer used for measurement, which has not been considered up to date. With this aim in mind, aptamers raised against the neutrophil gelatinase–associated lipocalin (NGAL or lipocalin-2) protein were selected [10] because i) this protein has been proposed as a potential biomarker for pancreatic adenocarcinoma (PADC) and hepatocellular carcinoma in combination with other biomarkers [10-12]; ii) they are one of the few examples of a pair of aptamers reported for a given target even though the selection procedure, SELEX, provides dozens of potential receptors and iii) the described pM dissociation constant of the aptamer-ligand interaction.

Thorough characterization of aptamer-target interaction is the last but the most important step in the selection process. It provides invaluable information such as binding affinity and minimum sequence required for tight binding. However, it is not an easy task because characterization of aptamer-ligand complexes is highly dependent on the nature and sensitivity of the technique selected, which frequently render overestimated apparent affinities. Many different techniques based on kinetics or equilibrium analysis have been used [13]; most of them require labeling and/or immobilization, which can alter the affinity. Heterogeneous or surface-phase affinity are

also affected by the interaction model employed, typically Langmuir model, though more sophisticated models are usually operating due to immobilization-dependent receptor crowding that limits the target accessibility, binding-site heterogeneity, avidity or allosteric effects [14-16]. Discrepancies larger than two orders of magnitude for small molecules such as tobramycin [17] or proteins such as thrombin [18] advise to use more than one method to evaluate the affinity.

In this work two different anti-NGAL aptamers were used in direct, sandwich and competitive assay formats on Au electrodes and magnetic beads. For improved detection, a rolling circle signal amplification was designed and carefully optimized and applied to the different formats using a truncated 40-nt aptamer. We have shown the shortened aptamer version retains comparable affinity to the full length sequence. The direct aptamer binding to protein can be observed at aptamer concentrations as low as 15 pM, three orders of magnitude lower than with conventional enzyme amplification. Aptamers do not behave equally well in different assays [19]. This was apparent when sandwich and competitive assays were developed. Fueled by these contradictory results, further characterization by SPR and microscale thermophoresis was accomplished that totally explained the analytical results.

## Materials and methods

Materials and instrumentation can be found in Supplementary Material. Magnetic beads (MBs), screen-printed gold electrode (SPAuE) and Au disc modification protocols are compiled in Experimental Protocols section in Supplementary Material.

**Sandwich assay on Au electrodes**

The SPAuE modified with the mixed DNA-*p*-aminothiophenol self-assembled monolayer (DNA-*p*-ATP SAM) was incubated with 50 µL of 500 ng $mL^{-1}$ NGAL in 1× PBS containing 0.5% BSA for 1 h. After washing with that buffer and drying with $N_2$,

0.5 or 0.1 µM of LCN2-2R aptamer was added for 1 h at room temperature (RT) unless otherwise stated. The labeling step was carried out with peroxidase conjugated to a Fab-anti-FITC (antiFITC-POD) diluted at 0.5 U $mL^{-1}$ in 1× PBS with 0.5% casein (w/v) as a blocking agent. This solution was dropped on the electrochemical cell and incubated for 30 min at RT and protected from light. After washing with 1× PBS, the cell was covered with 35 µL of the substrate solution for 30 s and immediately chronoamperometry was performed at 0 V for 60 s.

**Direct assay on Au electrodes**

Increasing concentrations of LCN2-2R in 1× PBS were incubated on the NGAL-modified SPAuE surface for 30 min and washed out with 1× PBS. Labeling and detection steps were carried out as indicated above.

**RCA detection on SPAuE**

The working electrode modified with the mixed *p*-ATP SAM was covered with a solution containing 10 nM padlock and 0.125 Weiss $µL^{-1}$ T4 DNA ligase in 1× ligase buffer for 30 min at RT to allow padlock hybridization and circularization (Fig. S1). The reaction was stopped by removing the solution and washing with 1× PBS. The rolling circle amplification was performed in a solution containing 0.25 U $µL^{-1}$ phi29 polymerase and 0.5 mM dNTPs in the 1× polymerase buffer for 15 min at 37 °C in an oven. After thorough washing with 1× PBS, a 10 µL drop of 100 nM reporter probe in 1× PBS was added to the working electrode and incubated for 30 min at RT protected from light. Then, the enzyme labeling step, the enzymatic reaction and chronoamperometric detection were carried out as indicated above.

**Direct assay on modified MBs**

60 µg of NGAL-modified MBs were incubated in 250 µL of increasing concentrations of signaling aptamer, LCN2-2Rt or LCN2-2RCA, in 1× PBS (0.5 pM –

500 nM) for 30 min. (Fig. 1, step 1). After removing the supernatant with magnetic entrapment, the MBs were washed twice with PBS-0.01 % Tween20 (washing buffer).

**Preferred place for Fig. 1.**

When RCA was not used for detection, the next step was the enzyme labeling with antiFITC-POD prepared as indicated above for 30 min (Fig. 1, step 5). After two washing steps with washing buffer and one without Tween20, the MBs were resuspended in 30 µL of 1× PBS. 10 µL of MBs were dropped on the working electrode and entrapped magnetically for 1 min with the help of a magnet under it (Fig. 1, step 6). Finally, 30 µL of the substrate solution were added and the enzymatic reaction proceeded for 30 s. Immediately after, chronoamperometry was performed at 0 V for 60 s. All incubations were carried out at RT under stirring.

When RCA was used for signal amplification, the MBs were resuspended in 30 µL of a solution containing 10 nM padlock and 0.125 Weiss $\mu L^{-1}$ T4 DNA ligase in 1× ligase buffer for 30 min at RT (Fig. 1, step 2) with agitation in the mixer wheel. After this, the supernatant was removed and MBs washed with washing buffer first and then in 1× PBS. The RCA was carried out in 30 µL of 0.5 mM dNTPs and 0.25 U $\mu L^{-1}$ phi29 DNA polymerase in 1× polymerase buffer for 15 min at 37 °C with agitation in Thermomixer (Fig. 1, step 3). Afterward, the supernatant was removed and the MBs were washed with washing buffer and 1× PBS. Then, the MBs were incubated in 250 µL of 100 nM reporter probe in 1× PBS for 30 min under agitation at RT in the mixer wheel (Fig. 1, step 4). After removing the supernatant and washing as previously, the enzymatic labeling (Fig. 1, step 5) and reaction as well as the chronoamperometric detection was carried out as indicated when no RCA was carried out (Fig. 1, step 6).

**Competitive assay on NGAL-modified MBs**

60 µg of NGAL-modified MBs were incubated in 250 µL of a solution containing 15 pM LCN2-2RCA and varying concentrations of human NGAL expressed in HEK 293 cells for 30 min at RT under agitation in the mixer wheel. The solution complex aptamer-NGAL was separated from the complex on the MBs by removing the supernatant. Two successive washing steps in washing buffer and PBS were finally performed before starting the RCA or the conventional enzyme signal amplification and detection as stated above.

**Sandwich assays on streptavidin-MBs**

First, 25 µL of capture aptamer-coated MBs were resuspended in 250 µL of NGAL solutions prepared in 1× PBS with 0.1% BSA, with target protein concentrations in the range 0 to 500 ng $mL^{-1}$. The protein incubation proceeded for 30 min at 25 °C under constant stirring in the Thermomixer. Then, the MBs were washed twice with 1× PBS+0.01% Tween 20 (washing buffer), resuspended in 250 µL of 100 nM reporter aptamer (LCN2-2Rt for symmetrical and normal configurations or LCN2-4Ctb for inverted configuration) in 1× PBS and incubated for 30 min at 25 °C under shaking in the Thermomixer. After two washings with washing buffer, the enzymatic labeling was performed by resuspending the beads in 250 µL of either antiFITC-POD conjugate (0.5 U $mL^{-1}$ prepared in casein blocking buffer 0.5% in 1× PBS) or streptavidin-POD conjugate ($4\times10^{-3}$ g $L^{-1}$ prepared in 5× SSPE containing 2% BSA and 0.005% Tween 20, corresponding to 0.5 U $mL^{-1}$ of POD) depending on the reporter aptamer tag, 6-carboxyfluorescein (6-FAM) or biotin. The resulting suspension was incubated for 30 minutes at 25 °C under constant stirring. After that, the beads were sequentially washed twice with washing buffer and once with 1× PBS, and finally reconstituted in 25 µL of

1× PBS. The enzymatic reaction and the chronoamperometric measurement were carried out as mentioned above.

**NGAL-aptamer affinity by SPR measurements**

An NGAL-modified Au sensor disc was used to study the affinity of LCN2-2Rt aptamer in 1× PBS (running buffer). Each independent binding experiment includes baseline, association and dissociation steps as follows. After obtaining a stable signal by acquiring several baselines in running buffer, varying concentrations of aptamer prepared in 1× PBS (35 µL) were injected in one channel while only the running buffer in the reference channel and the association phase was recorded for 10 min. After draining the cuvettes, 50 µL of 1× PBS were injected and the dissociation phase was monitored for 5 min resulting in a decrease of the resonance angle until a stable value was achieved due to loss of the weakly bound aptamer. The difference between the resonance angle in m° after and before the association step is a measurement of the amount of aptamer bound specifically to NGAL provided that the corresponding signal registered in the reference channel is subtracted. All steps were recorded under needle-based agitation to avoid mass transfer control of reaction kinetics.

## Results and discussion

**SPAuE aptamer-based assays**

Initial experiments using the previously described aptamers as capture (LCN2-4C) and signaling receptors (LCN2-2R) in a sandwich format using conventional enzyme amplification showed very high currents in the absence of NGAL even after blocking with 0.5 % BSA (Fig. S2). Those signals were not related to the enzyme conjugate unspecific adsorption that showed low currents 148(± 17) nA. The feasibility of a stable hybridization between both aptamers was investigated using Mfold web server [20]. A

Gibbs free energy (ΔG) of -10.3 kcal/mol was obtained at 25 °C and [$Na^+$]=0.3 M for the aptamers hybridization. This value is close to the reported value to cause strong blank currents in genoassays [21]. This theoretical finding along with a dramatic decrease in the blank current when the incubation of the signaling aptamer was carried out at 40 °C in an oven points to this undesired hybridization as the more plausible explanation. Unfortunately, the signal for 500 ng $mL^{-1}$ NGAL also decreases.

Difficult formation of the three-component sandwich complex has been reported with the widely used thrombin aptamers due to displacement of the protein towards the aptamer in solution. Pre-formed secondary aptamer-protein complex alleviates this issue that is further improved when the enzyme-conjugate is also pre-associated in a single step sandwich assay [18]. Interestingly, the sandwich assay developed by Lee et al. uses a capture aptamer covalently attached to microtiter plates and an enzyme-labeled aptamer [10], an uncommon modification taking into account that the bulky enzyme might impede proper aptamer-ligand recognition. In order to verify whether this strategy could minimize hybridization while maintaining the aptamer affinity, two different sandwich constructions were assayed: i) a two steps format, that is, NGAL incubation on the electrode surface followed by addition of the signaling aptamer-enzyme conjugate pre-associated complex or ii) a single step format, i.e: incubation of NGAL and signaling aptamer in solution and subsequent addition of enzyme conjugate in order not to perturb the recognition event and application of the three component assembly onto the modified SPAuE. Both strategies yielded low unspecific but also specific signals that are virtually identical within the experimental error (Fig. S2). Taken together, these experiments shed a shadow on the actual affinity of NGAL aptamers described as extremely high; $6.09 \cdot 10^{-11}$ M and $2.24 \cdot 10^{-12}$ M for capture and signaling aptamers, respectively [10].

The affinity of the signaling aptamer was examined in a direct assay. Aptamer binding curves to NGAL covalently bound to a pure SAM of *p*-mercaptobenzoic acid (*p*-MBA) were recorded at different NGAL coverage achieved from solutions containing between 10 and 35 µg $mL^{-1}$ using the recombinant protein expressed in bacteria (not glycosylated) or in HEK human cells (glycosylated). In both cases, the best results were obtained using 25 µg $mL^{-1}$ of the protein during the immobilization step (Fig. 2).

**Preferred place for Fig. 2.**

Larger amounts of immobilized protein are detrimental for the reproducibility while smaller ones only showed significant responses at the highest aptamer concentration (data not shown). Interestingly, saturation currents are low (~300 nA) for bacterial NGAL and even lower (~200 nA) for the human protein but reached at smaller aptamer concentrations, which indicates a slightly better affinity for the glycosylated form. This result is reasonable because the selection was performed against a protein expressed in human cells [10], so in subsequent studies the glycosylated NGAL was used. Interestingly, similar currents were obtained with a truncated version of signaling aptamer, LCN2-2Rt, only containing the 40 nt central region, which reveals that primers are not essential for the recognition even though they were not trimmed in previous work.

**Rolling circle amplified direct NGAL recognition**

Isothermal amplification schemes can be employed in combination with aptamers to improve detectability. With this aim, a RCA step was designed and optimized using the complete thiolated capture aptamer chemisorbed on SPAuE as in previous studies. The RCA requires three steps: i) padlock hybridization to the primer; ii) padlock

ligation (circularization) and iii) padlock amplification. Then hybridization with a 6-FAM-labeled DNA reporter probe followed by enzyme labeling and chronoamperometric measurements were performed (Fig. S1). Preliminary experiments showed significant differences between the blank (absence of padlock), 160 (±3) nA, and 100 nM padlock, 3.4 (±1.8) µA. Improved results were obtained when the padlock hybridization and ligation were carried out in a single step, 17.9 (±0.8) µM with blank currents of 202 (±44) nA, shortening the assay, so in subsequent experiments both steps were performed together. The very high currents suggest that some experimental conditions can be optimized to reduce the cost and the assay time. The ligase, phi29 polymerase, padlock and reporter probe concentrations as well as the hybridization-ligation, amplification, reporter hybridization and enzyme-conjugate incubation times were optimized. In Fig. 3 currents obtained under several conditions with and without the padlock are shown as well as the corresponding signal to blank ratio (S/B). Ligase and polymerase buffers contain DTT at high concentrations that are known to displace chemisorbed oligonucleotides from the surface, so decreasing the concentration and interaction time was beneficial in terms of specific analytical signal.

After these modifications, the highest S/B ratio was obtained (column 4). Nonetheless, currents were still high, so further optimization was tested. The most influential parameter on the analytical signal was the reporter probe concentration that was finally established at 100 nM. A trade-off between S/B ratio, assay time and consumption of reagents were the criteria to select the final conditions indicated in Table S3. Under optimized conditions, RCA and labeling steps can be completed within 90 min instead of the initial 4.5 h. To the best of our knowledge, none RCA based assay has shortened the amplification step to only 15 min. In a particular assay where the elongated sequence has a strong secondary structure (G-quartets) to work as a

DNAzyme, the length of RCA was shortened to 20 min to minimize strong intra- or interchain interactions deleterious to the DNAzyme performance [22]. In immunoRCA a 30 min step was selected as optimum time [23].

**Preferred place for Fig. 3.**

One could speculate that direct recognition of NGAL on the aptamer-modified SPAuE would hinder the RCA amplification. However, comparable high currents were observed in the presence and in the absence of 500 ng $mL^{-1}$ human NGAL. This indicates that capture aptamer has a low affinity for its ligand or the 5'-end primer is not involved in the recognition, so RCA can take place without restriction.

The optimized RCA was then challenged to the recognition of NGAL immobilized on tosylactivated magnetic beads (direct assay) using a truncated signaling aptamer (LCN2-2RCA) that contains 40-nt aptamer and the reverse primer separated with a 10-thymine spacer to ensure that binding to the protein does not perturb the padlock hybridization (Fig. 1). The direct assay with increasing concentrations of aptamer is depicted in Fig. 4.

For comparison, the non-RCA amplified binding curve using the truncated signaling aptamer without primers (LCN2-2Rt) is also included. A large displacement toward lower aptamer concentrations is apparent with RCA. Fitting curves to a logistic model (eq. 1), where A is the response at infinite concentration of aptamer, B is the response to 0 concentration of aptamer both in µA, $IC_{50}$ is the aptamer concentration giving a 50% reduction of the maximum signal in nM and p is the Hill slope that represents the slope at the inflection point,

$$y = \frac{B-A}{1+\left(\frac{x}{IC_{50}}\right)^{p}} + A \qquad \text{(eq. 1)}$$

give $IC_{50}$ values of 14(±3) pM and 10(±5) nM for the RCA amplified and non-RCA amplified methods. These values can be interpreted as an estimation of the apparent dissociation constant ($K_D$) assuming that the current is a measurement of bound aptamer. The thermodynamic $K_D$ cannot depend on the particular approach especially when chronoamperometry is performed in both studies. This means that the $K_D$ values are a measurement of the stability of the overall architecture of the assay i.e. its functional affinity. In any case, estimated values are one and three orders of magnitude higher than the previously reported using SPR in an analogue immobilization set-up, that is, protein covalently linked to the surface. In that case, the complete 76-nt long aptamer was used but we have not found significant differences with the truncated version as mentioned above.

Selectivity of the aptamer was tested using MBs modified with BSA or PSA. Currents similar to the blank were obtained in the whole range (Fig. 4) confirming the selective recognition of NGAL by the truncated aptamer.

**Preferred place for Fig. 4.**

**NGAL aptaassays on MBs**

A competitive assay using NGAL-modified MBs and a mixture of a fixed concentration of aptamer set at the $IC_{50}$ and 50-500 nM glycosylated NGAL in solution (Fig. 5A) was tested. A small decrease in the current was observed with increasing concentrations of protein but the short range did not allow the assay development. The lack of competition cannot be attributed to RCA artifacts because similar trend was obtained without RCA.

**Preferred place for Fig. 5.**

Alternatively, sandwich assays on streptavidin-modified MBs with truncated aptamers were also tried. Since signaling aptamer showed some affinity for the target,

we first prepared MBs with biotinylated (LCN2-2Rtb) and 6-FAM-tagged (LCN2-2Rt) signaling aptamer as a capture and secondary receptors, respectively, a "symmetric" configuration where both aptamers are identical. Different aptamers were also assayed as capture and secondary aptamers in a normal (LCN2-4Ctb and LCN2-2Rt) and inverted configuration (LCN2-2Rtb and LCN2-4Ctb) with respect to the previously reported [10]. Biotinylated aptamers were designed with a $T_{10}$ spacer to ensure proper recognition and minimize steric hindrance on the MB surface. Potential deleterious hybridization was checked, obtaining $\Delta G$ values below -10 kcal $mol^{-1}$ in all combinations, which reduces the chance of large unspecific currents. Data depicted in Fig. 5B indicates that the currents in the presence and in the absence of 250 ng $mL^{-1}$ NGAL are virtually identical in all cases where no RCA amplification was carried out. In the symmetric configuration, two identical binding sites in the protein are required, so their absence can account for the negligible response. However, when the assay was RCA amplified a small difference is apparent suggesting those sites are indeed present. The normal experiment was carried out with MBs modified with LCN2-4Ctb in a high salt solution (1 M NaCl and 0.5 mM EDTA in 5 mM Tris-HCl) to increase the number of receptors immobilized on the surface but it did not yield better results, which confirms the low affinity of both aptamers for the protein.

**Signaling aptamer characterization**

In order to independently verify the affinity of the aptamers, SPR and microscale thermophoresis analysis were carried out. Mixed SAMs of mercaptoundecanoic acid/mercaptohexanol 1:3 were prepared on SPR sensor chips to covalently immobilize the NGAL up to a response change of 150-200 mº to ensure a full monolayer of protein

but excluding multilayers that could preclude the interaction with the aptamer (Fig. S3A).

The predicted maximum response change upon saturation of the monolayer with aptamer was calculated to be 100-140 mº by eq. 2 [24],

$$A_{pred} = A_{NGAL} \frac{MW_{apt}}{MW_{NGAL}} \frac{RII_{apt}}{RII_{NGAL}} \qquad \text{eq. 2}$$

where $A_{pred}$ and $A_{NGAL}$ are the predicted and the measured changes in resonance angle units due to the binding of aptamer and NGAL on the surface, respectively, and RII is the average refractive index increment due to the presence of aptamer and NGAL.

Under those conditions, only when 1 µM of LCN2-2Rt was incubated in the SPR cuvette, a clear binding kinetics is recorded during the association step while a decrease is apparent due to removal of the weakly bound aptamer but the signal does not reach the baseline value, which is a clear indication of a specific binding to the protein (Fig. S3B). In contrast, in the reference channel, after a vertical shift related to the injection, the signal returns to the baseline indicating that there is no aptamer in solution. The average change of three independent measurements was 27 mº; between 19 and 27% of the predicted value. This means that, even at µM level, saturation is not achieved, pointing out again to a poor affinity. Similar experiments using the capture aptamer (LCN2-4C) did not give any specific signal suggesting even lower affinity than the signaling aptamer.

In order to ascertain whether the immobilization on Au surfaces causes affinity degradation, a technique that measures the thermodynamic dissociation constant in solution was used. Microscale thermophoresis (MST) analysis failed to obtain a binding curve in the nM range using a fixed concentration of fluorescein-tagged signaling aptamer (LCN2-2Rt) and increasing concentrations of NGAL up to 1.2 µM (20-fold the aptamer concentration). Higher concentrations were not studied due to limitation in the

amount of protein available. Initial fluorescence measurement starts increasing at concentrations above 0.1 µM of protein (Fig. S4A). A control experiment under denaturing conditions (4% SDS and 40 mM DTT in PBS) shows identical results suggesting that processes not related to aptamer binding such as aggregation or adsorption are operating. A titration in the presence of 0.05% Tween20 and 0.2% BSA to avoid adsorption failed to detect any binding (Fig. S4, B-D). MST experiments confirm the low affinity of signaling aptamer for the target in solution and might explain the absence of competition between NGAL in solution and immobilized on MBs. Under certain conditions, improved heterogeneous binding affinity has been described with favorable aptamer presentation or avidity as plausible explanations [16, 25]. In the anti-NGAL aptamer case, when a high local concentration of the protein as those achieved on MBs is used, binding is clearly observed though at nM instead of pM aptamer concentrations. With smaller local concentrations as those in solution there is no apparent binding, which explains the lack of competition in the protein concentration range we assayed. The small positive signal in the symmetric sandwich assay coupled to RCA suggests that two binding sites for, at least, LCN2-2 aptamer exist, so avidity effects cannot be excluded.

## Conclusions

The characterization of the binding interaction of new aptamers to their cognate targets under operational conditions contributes to broad their application field. In this work, we demonstrate that a truncated anti-NGAL aptamer remains as functional as the longer counterpart previously reported in the literature. Optimization of a RCA elongation reaction coupled to the aptamer recognition lead to a three orders of magnitude of amplification signal when compared to conventional single enzymatic

detection, a parameter usually not provided in the literature. The DNA elongation step is shortened to only 15 min and consumption of expensive enzymes was also cut to a minimum obtaining sensitive enough electrochemical signals, which could make affordable the use of molecular biology tools in biosensors. However, surprisingly this improvement is not reflected in the analytical performance of competitive assays. The aptamer affinity characterization toward its target protein by SPR and microscale thermophoresis revealed an apparent and significant overestimation of its affinity in previous work. This result emphasize the importance of the solution-phase affinity in competitive assays, which is not commonly estimated and can be significantly different from the surface-confined one accounting for flawed assays. In such cases, the benefits from the improved functional affinity achieved by RCA amplification are apparent in direct assays but cannot be fully counterbalanced when the solution-phase affinity is rather poor as the case for antiNGAL aptamers according to MST measurements.

Taken together our results strongly advise to use several techniques to fully characterize aptamer not only to validate the potential usefulness but also to find the minimal sequence needed. Otherwise, unreliable or poor performance aptamers will be derived, not adequate to the extreme sensitivity required for cancer biomarker detection.

## Acknowledgments

R.L.G thanks the Spanish Ministerio de Educación, Cultura y Deporte for the FPU grant (FPU16/05670). This work was financially supported by the Spanish Ministerio de Economía, Industria y Competitividad (Project No. CTQ2015-63567-R), and co-financed by FEDER funds.

## Appendix A. Supplementary material

Supplementary material associated with this article can be found in the online version.

## References

[1] J.D. Cohen, A.A. Javed, C. Thoburn, F. Wong, J. Tie, P. Gibbs, C.M. Schmidt, M.T. Yip-Schneider, P.J. Allen, M. Schattner, R.E. Brand, A.D. Singhi, G.M. Petersen, S.M. Hong, S.C. Kim, M. Falconi, C. Doglioni, M.J. Weiss, N. Ahuja, J. He, M.A. Makary, A. Maitra, S.M. Hanash, M. Dal Molin, Y. Wang, L. Li, J. Ptak, L. Dobbyn, J. Schaefer, N. Silliman, M. Popoli, M.G. Goggins, R.H. Hruban, C.L. Wolfgang, A.P. Klein, C. Tomasetti, N. Papadopoulos, K.W. Kinzler, B. Vogelstein, A.M. Lennon, Combined circulating tumor DNA and protein biomarker-based liquid biopsy for the earlier detection of pancreatic cancers, Proc Natl Acad Sci U S A, 114 (2017) 10202-10207.

[2] J.D. Cohen, L. Li, Y. Wang, C. Thoburn, B. Afsari, L. Danilova, C. Douville, A.A. Javed, F. Wong, A. Mattox, R.H. Hruban, C.L. Wolfgang, M.G. Goggins, M. Dal Molin, T.L. Wang, R. Roden, A.P. Klein, J. Ptak, L. Dobbyn, J. Schaefer, N. Silliman, M. Popoli, J.T. Vogelstein, J.D. Browne, R.E. Schoen, R.E. Brand, J. Tie, P. Gibbs, H.L. Wong, A.S. Mansfield, J. Jen, S.M. Hanash, M. Falconi, P.J. Allen, S. Zhou, C. Bettegowda, L.A. Diaz, Jr., C. Tomasetti, K.W. Kinzler, B. Vogelstein, A.M. Lennon, N. Papadopoulos, Detection and localization of surgically resectable cancers with a multi-analyte blood test, Science, 359 (2018) 926-930.

[3] A.K. Fuzery, J. Levin, M.M. Chan, D.W. Chan, Translation of proteomic biomarkers into FDA approved cancer diagnostics: issues and challenges, Clin Proteom, 10 (2013).

[4] A. Mordente, E. Meucci, G.E. Martorana, A. Silvestrini, Cancer Biomarkers Discovery and Validation: State of the Art, Problems and Future Perspectives, in: R. Scatena (Ed.) Advances in Cancer Biomarkers Springer Dordrecht Heidelberg, New York, 2015, pp. 9-26.

[5] U. Kuzmanov, H. Kosanam, E.P. Diamandis, The sweet and sour of serological glycoprotein tumor biomarker quantification, BMC medicine, 11 (2013) 31.

[6] L. Zhang, S. Wan, Y. Jiang, Y. Wang, T. Fu, Q. Liu, Z. Cao, L. Qiu, W. Tan, Molecular Elucidation of Disease Biomarkers at the Interface of Chemistry and Biology, J Am Chem Soc, 139 (2017) 2532-2540.

[7] D. Xiang, S. Shigdar, G. Qiao, T. Wang, A.Z. Kouzani, S.F. Zhou, L. Kong, Y. Li, C. Pu, W. Duan, Nucleic acid aptamer-guided cancer therapeutics and diagnostics: the next generation of cancer medicine, Theranostics, 5 (2015) 23-42.

[8] C. Feng, X.X. Mao, Y.C. Yang, X.L. Zhu, Y.M. Yin, G.X. Li, Rolling circle amplification in electrochemical biosensor with biomedical applications, J. Electroanal. Chem, 781 (2016) 223-232.

[9] Y. Zhu, H.J. Wang, L. Wang, J. Zhu, W. Jiang, Cascade Signal Amplification Based on Copper Nanoparticle-Reported Rolling Circle Amplification for Ultrasensitive Electrochemical Detection of the Prostate Cancer Biomarker, Acs Applied Materials & Interfaces, 8 (2016) 2573-2581.

[10] K.-A. Lee, J.-Y. Ahn, S.-H. Lee, S.S. Sekhon, D.-G. Kim, J. Min, Y.-H. Kim, Aptamer-based Sandwich Assay and its Clinical Outlooks for Detecting Lipocalin-2 in Hepatocellular Carcinoma (HCC), Sci Rep, 5:10897 (2015).

[11] N. Moniaux, S. Chakraborty, M. Yalniz, J. Gonzalez, V.K. Shostrom, J. Standop, S.M. Lele, M. Ouellette, P.M. Pour, A.R. Sasson, R.E. Brand, M.A. Hollingsworth, M. Jain, S.K. Batra, Early diagnosis of pancreatic cancer: neutrophil gelatinase-associated lipocalin as a marker of pancreatic intraepithelial neoplasia, Br J Cancer, 98 (2008) 1540-1547.

[12] Z. Tong, A.B. Kunnumakkara, H. Wang, Y. Matsuo, P. Diagaradjane, K.B. Harikumar, V. Ramachandran, B. Sung, A. Chakraborty, R.S. Bresalier, C. Logsdon,

B.B. Aggarwal, S. Krishnan, S. Guha, Neutrophil gelatinase-associated lipocalin: a novel suppressor of invasion and angiogenesis in pancreatic cancer, Cancer Res, 68 (2008) 6100-6108.

[13] R. Miranda-Castro, N. de-los-Santos-Álvarez, M.J. Lobo-Castañón, Characterization of aptamer-ligand complexes, in: Y. Dong (Ed.) Aptamers for analytical applications: Affinity optimization and method design, Wiley VCH Verlag GmbH, 2018.

[14] S. Amaya-González, L. López-López, R. Miranda-Castro, N. de-los-Santos-Álvarez, A.J. Miranda-Ordieres, M.J. Lobo-Castañón, Affinity of aptamers binding 33-mer gliadin peptide and gluten proteins: Influence of immobilization and labeling tags, Anal. Chim. Acta, 873 (2015) 63-70.

[15] C. Daniel, Y. Roupioz, D. Gasparutto, T. Livache, A. Buhot, Solution-phase vs surface-phase aptamer-protein affinity from a label-free kinetic biosensor, Plos One, 8 (2013) e75419.

[16] R. Stoltenburg, T. Schubert, B. Strehlitz, In vitro Selection and Interaction Studies of a DNA Aptamer Targeting Protein A, Plos One, 10 (2015) e0134403.

[17] J. Fuchs, J.B. Fiche, A. Buhot, R. Calemczuk, T. Livache, Salt concentration effects on equilibrium melting curves from DNA microarrays, Biophys J, 99 (2010) 1886-1895.

[18] C. Daniel, F. Melaine, Y. Roupioz, T. Livache, A. Buhot, Real time monitoring of thrombin interactions with its aptamers: insights into the sandwich complex formation, Biosens Bioelectron, 40 (2013) 186-192.

[19] N. Li, J.N. Ebright, G.M. Stovall, X. Chen, H.H. Nguyen, A. Singh, A. Syrett, A.D. Ellington, Technical and biological issues relevant to cell typing with aptamers, J Proteome Res, 8 (2009) 2438-2448.

[20] M. Zuker, Mfold web server for nucleic acid folding and hybridization prediction, Nucleic Acids Res., 31 (2003) 3406-3415.

[21] R. Miranda-Castro, N. de-los-Santos-Álvarez, M.J. Lobo-Castañón, Understanding the factors affecting the analytical performance of sandwich-hybridization genosensors on gold electrodes, Electroanalysis, 30 (2018) 1229-1240.

[22] L. Tang, Y. Liu, M.M. Ali, D.K. Kang, W. Zhao, J. Li, Colorimetric and ultrasensitive bioassay based on a dual-amplification system using aptamer and DNAzyme, Anal Chem, 84 (2012) 4711-4717.

[23] B. Schweitzer, S. Wiltshire, J. Lambert, S. O'Malley, K. Kukanskis, Z. Zhu, S.F. Kingsmore, P.M. Lizardi, D.C. Ward, Immunoassays with rolling circle DNA amplification: a versatile platform for ultrasensitive antigen detection, Proc Natl Acad Sci U S A, 97 (2000) 10113-10119.

[24] T.M. Davis, W.D. Wilson, Determination of the Refractive Index Increments of Small Molecules for Correction of Surface Plasmon Resonance Data, Anal. Biochem., 284 (2000) 348-353.

[25] R.A. Potyrailo, R.C. Conrad, A.D. Ellington, G.M. Hieftje, Adapting selected nucleic acid ligands (aptamers) to biosensors, Anal. Chem., 70 (1998) 3419-3425.

CAPTIONS FOR THE FIGURES

**Fig. 1.** Schematic illustration of the protocols for the binding curves without (A) and with (B) rolling circle amplification on NGAL-modified MBs. Step 1: aptamer recognition, 2: padlock hybridization and ligation, 3: RCA, 4: reporter probe hybridization, 5: enzyme labeling, 6: MBs entrapment on SPCE, substrate addition, enzymatic reaction and chronoamperometric measurement.

**Fig. 2**. Direct assays on SPAuE modified with 35 µg/mL (black dot), 25 µg/mL (green dot) human NGAL expressed in *E. coli* and 25 µg/mL of human NGAL express in HEK 293 cell (red triangle). Currents were obtained by chronoamperometry with increasing concentrations of LCN2-4C aptamer in PBS for 30 min.

**Fig. 3.** Optimization of RCA on SPAuE using the LCN2-4C aptamer in a mixed SAM. Chronoamperometric currents in the presence (green) and the absence (pink, inset) of padlock are shown as well as the S/B ratio. Detailed conditions of each nine experiments are summarized in Table S2 in the supporting information.

**Fig. 4**. Direct assays currents obtained by chronoamperometry at 0 V using increasing concentrations of aptamer LCN2-2Rt on NGAL-modified MBs after enzyme (blue circle) or RCA signal amplification (green circle), and on BSA (open red circle) or PSA (open black triangle) modified MBs with RCA amplification. Fittings to a logistic equation are shown for NGAL assays.

**Fig. 5.** (A) Competitive assay on NGAL-modified MBs. Currents were obtained by chronoamperometry at 0 V in the presence of 15 pM of LCN2-2Rt aptamer and increasing concentrations of NGAL expressed in HEK 293 cells. (B) Sandwich assays on streptavidin-modified MBs under different configurations. Currents were obtained by chronomaperometry after incubation of 0 (violet) or 250 ng/mL NGAL expressed in HEK cells (green) and 100 nM secondary aptamer.

Figure 1

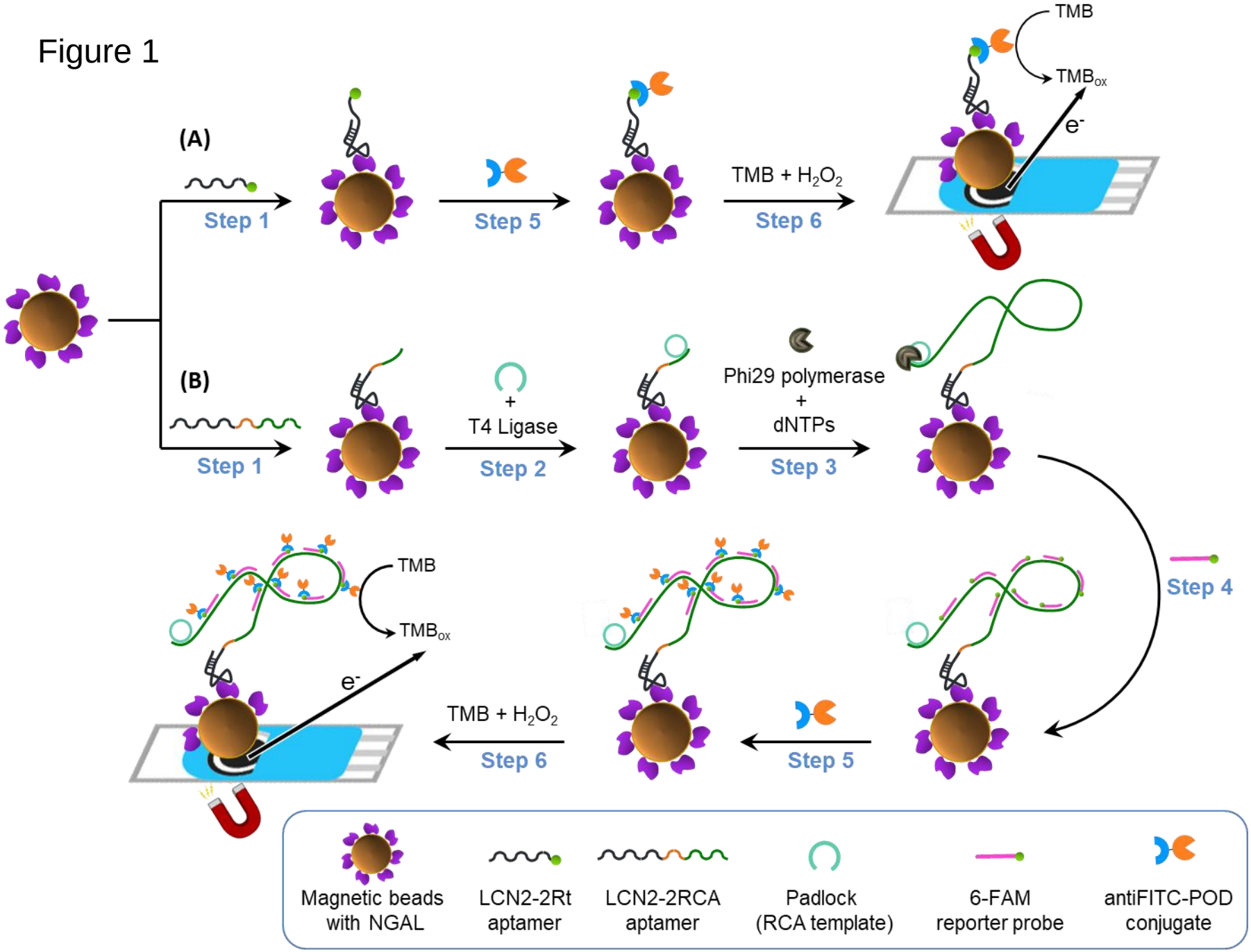
Figure 1
(A)
Step 1
Step 5
TMB + $H_2O_2$
Step 6
TMB
$TMB_{ox}$
$e^-$
(B)
Step 1
+
T4 Ligase
Step 2
Phi29 polymerase
+
dNTPs
Step 3
Step 4
Step 5
TMB + $H_2O_2$
Step 6
TMB
$TMB_{ox}$
$e^-$
Magnetic beads with NGAL
LCN2-2Rt aptamer
LCN2-2RCA aptamer
Padlock (RCA template)
6-FAM reporter probe
antiFITC-POD conjugate

# Figure 2

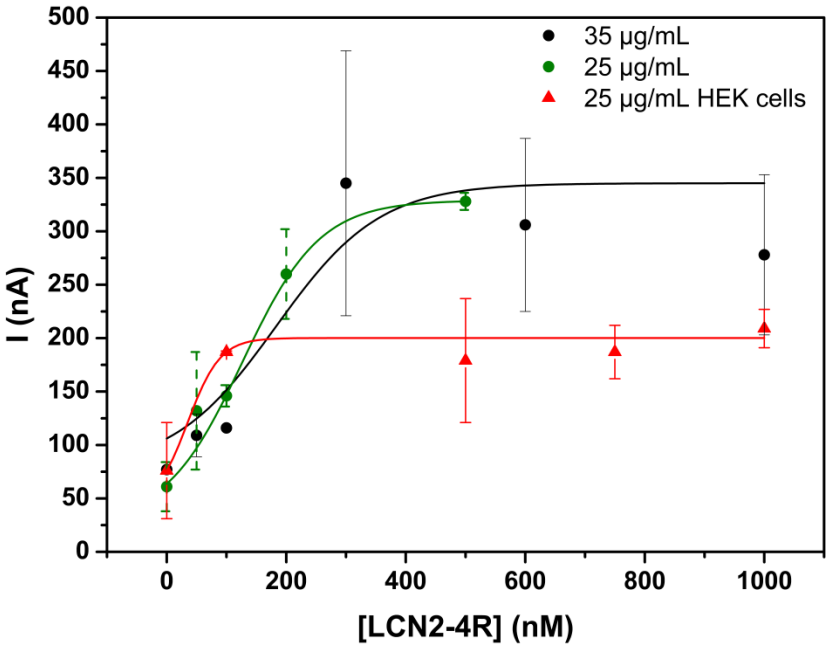
35 µg/mL
25 µg/mL
25 µg/mL HEK cells
I (nA)
[LCN2-4R] (nM)
0
50
100
150
200
250
300
350
400
450
500
0
200
400
600
800
1000

# Figure 3

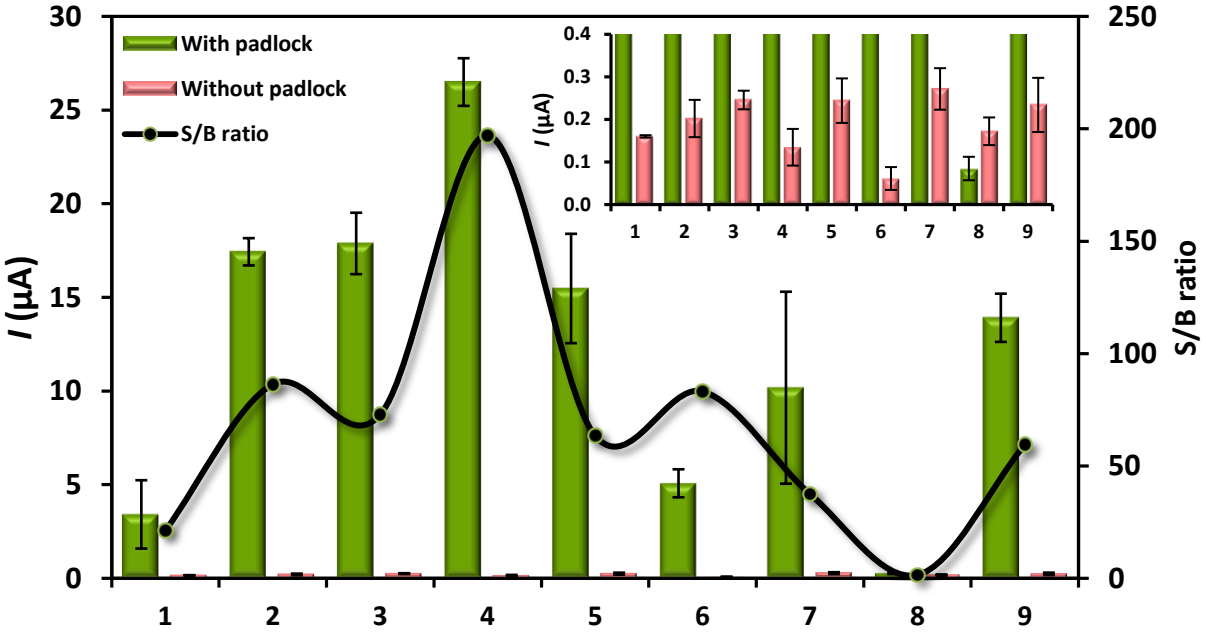
With padlock
Without padlock
S/B ratio
I (µA)
S/B ratio
30
25
20
15
10
5
0
250
200
150
100
50
0
1
2
3
4
5
6
7
8
9
0.4
0.3
0.2
0.1
0.0

**Figure 4**

# Figure 4

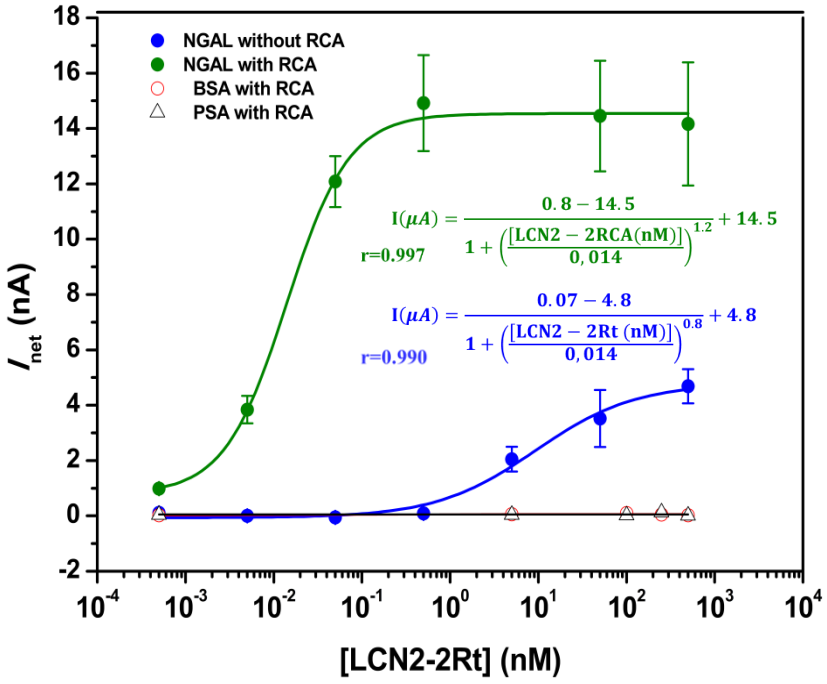

# Figure 5

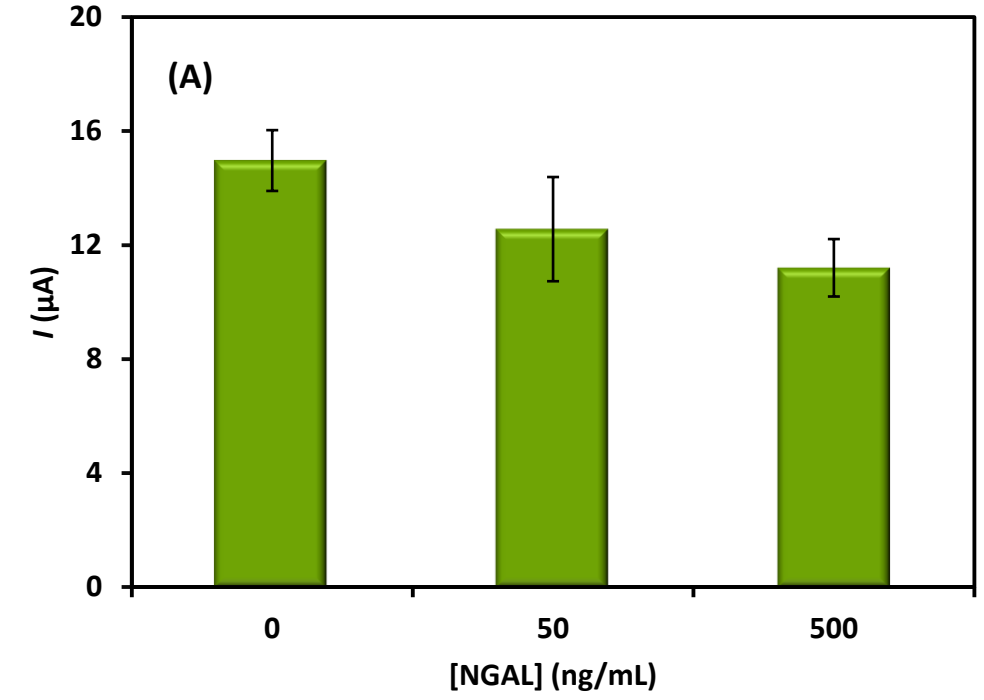
(A)
20
16
12
8
4
0
I (μA)
0
50
500
[NGAL] (ng/mL)

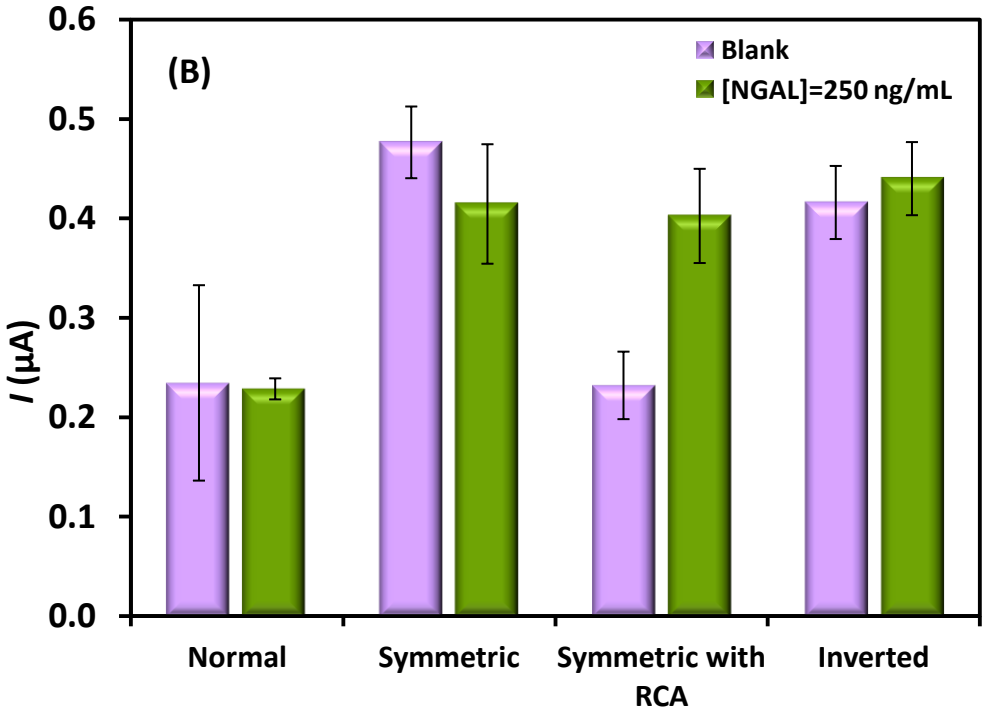
(B)
Blank
[NGAL]=250 ng/mL
0.6
0.5
0.4
0.3
0.2
0.1
0.0
I (μA)
Normal
Symmetric
Symmetric with RCA
Inverted

**Supplementary Material**

Click here to download Supplementary Material: Supplementary Information_UniOvi-revised.pdf